

Probing Scalar Nonstandard Interactions: Insights from the Protvino to Super-ORCA Experiment

Phys.Rev.D 109 (2024) 9, 095038

Dinesh Kumar Singha
University of Hyderabad

PPC 2024



- Neutrino mass states (ν_1, ν_2, ν_3) are related to flavour states by Unitary mixing matrix.

$$\text{Flavour States} \quad |\nu_\alpha\rangle = \sum_i U_{\alpha i} |\nu_i\rangle \quad \alpha = e, \mu, \tau, \quad i = 1, 2, 3 \quad \text{Mass States}$$

Potential CP violation $\sim \theta_{13}$

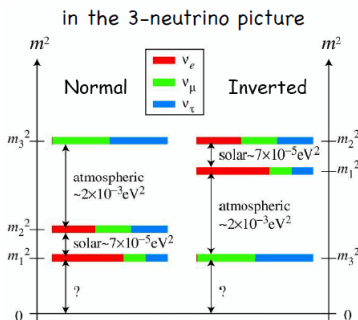
$$U_{\text{PMNS}} = \begin{pmatrix} 1 & 0 & 0 \\ 0 & c_{23} & s_{23} \\ 0 & -s_{23} & c_{23} \end{pmatrix} \begin{pmatrix} c_{13} & 0 & s_{13} e^{-i\delta} \\ 0 & 1 & 0 \\ -s_{13} e^{i\delta} & 0 & c_{13} \end{pmatrix} \begin{pmatrix} c_{12} & s_{12} & 0 \\ -s_{12} & c_{12} & 0 \\ 0 & 0 & 1 \end{pmatrix}$$

$(s_{ij} = \sin \theta_{ij}, \quad c_{ij} = \cos \theta_{ij})$



Unknowns in Neutrino Sector

Mass Hierarchy.



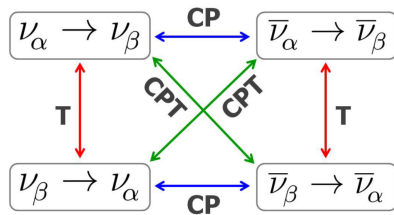
- $\Delta m_{31}^2 > 0$ (Normal Hierarchy)
 $m_3 \gg m_2 > m_1$
 - $\Delta m_{31}^2 < 0$ (Inverted Hierarchy)
 $m_2 > m_1 \gg m_3$
- * R. N. Mohapatra et al., arXiv:hep-ph/0510213

- Absolute scale of neutrino mass is unknown to us.
- Nature of Neutrinos: **Dirac** or **Majorana** type?

Unknowns in Neutrino Sector

$C[\text{Particle}] = \text{Antiparticle}$

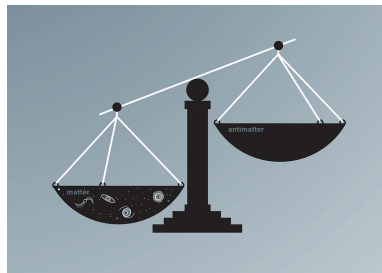
Parity changes the helicity of a state.



CP Violation

Is $P(\nu_\alpha \rightarrow \nu_\beta) \neq P(\bar{\nu}_\alpha \rightarrow \bar{\nu}_\beta)$?

- CP non-invariance comes from δ_{CP} phase in the Leptonic mixing matrix U .



- CP violation can explain the matter antimatter asymmetry in the universe.

*A. S. Joshipura et al. JHEP 08 (2001), 029

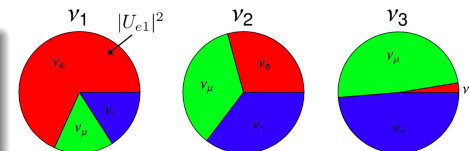
Unknowns in Neutrino Sector

Octant of θ_{23}

- Atmospheric mixing angle (θ_{23}) deviates from maximum-mixing value 45°

$\theta_{23} < 45^\circ$ Lower Octant (LO)

$\theta_{23} > 45^\circ$ Higher Octant (HO)



Is there more ν_μ or ν_τ in ν_3 ?

- Are there more than 3 neutrino mass eigenstates?
(Do sterile neutrinos exist?)
- Do neutrinos break the CPT and Lorentz invariance?
- Are there Non-Standard Interaction (NSI) effects?

- Neutrino oscillations → opportunity for new physics
- NSI of ν 's with matter is widely studied BSM physics in neutrino oscillations
- Two kinds of NSI in matter
 - Vector NSI: $\mathcal{L}_{NSI} = -2\sqrt{2}G_F \epsilon_{\alpha\beta}^{fC} (\bar{\nu}_\alpha \gamma^\mu P_L \nu_\beta)(\bar{f} \gamma_\mu P_C f)$,
 - Scalar NSI: $\mathcal{L}_{SNSI} = \frac{y_f Y_{\alpha\beta}}{m_\phi^2} (\bar{\nu}_\alpha \nu_\beta)(\bar{f} f)$,
- In matter vector NSI mainly comes with standard matter effect term
 $\Rightarrow H \sim M^2/2E + (V_{SI} + V_{NSI})$
- But the scalar NSI term modifies the mass matrix instead
 $\Rightarrow H \sim \frac{(M+\delta M)(M+\delta M)^\dagger}{2E} + V_{SI}$
- In model independent way, we can write this contribution as
 $\Rightarrow \delta M = \sqrt{|\Delta m_{31}^2|} \begin{pmatrix} \eta_{ee} & \eta_{e\mu} & \eta_{e\tau} \\ \eta_{e\mu}^* & \eta_{\mu\mu} & \eta_{\mu\tau} \\ \eta_{e\tau}^* & \eta_{\mu\tau}^* & \eta_{\tau\tau} \end{pmatrix}$
- P2SO and DUNE are the two longest possible neutrino oscillation experiments

Long-baseline options at KM3NeT: P2O, upgraded P2O, P2SO



Long-baseline options:

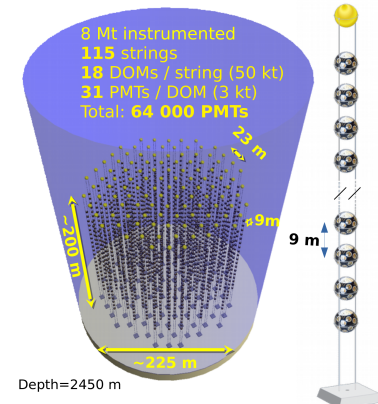
Neutrino source: U-70 synchrotron at Protvino

Baseline: 2595 km

Detector options: ORCA, Super-ORCA

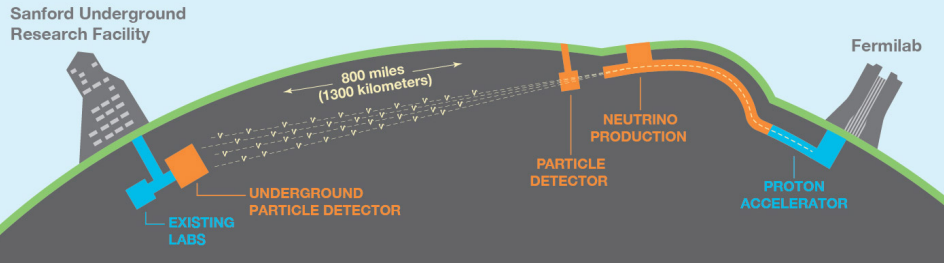
- ① P2O: Beam power \Rightarrow 90 KW, Detector \Rightarrow ORCA.
- ② upgraded P2O: Beam power \Rightarrow 450 KW, Detector \Rightarrow ORCA.
- ③ P2SO: Beam power \Rightarrow 450 KW, Detector \Rightarrow Super-ORCA.

Run time: 3 years ν + 3 years $\bar{\nu}$



* A. V. Akhmedov et al. Eur. Phys. J. C 79 (2019), no. 9 758. [arXiv:1902.06083].

Deep Underground Neutrino Experiment (DUNE)



- Future Long-Baseline experiment with a baseline of 1300 km.
- The neutrino source will be located at Fermilab, USA and the detector will be located in South Dakota, USA.
- Detects neutrinos of beam power 1.2 MW equivalent to 1.1×10^{21} POT per year with a 40 kt liquid argon time-projection chamber detector.
- Run-time into 3.5 years in ν mode and 3.5 years in $\bar{\nu}$ mode.



B. Abi et al. [DUNE], [arXiv:2103.04797 [hep-ex]].

Probability Plots

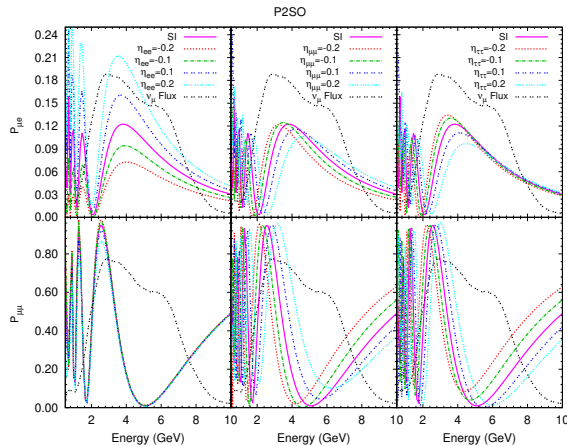


Figure: Appearance and disappearance probabilities for P2SO experiment.

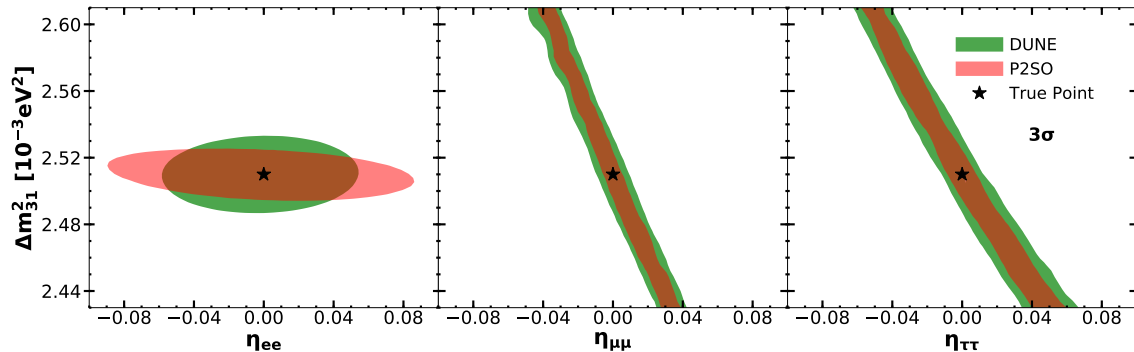
Allowed region of Δm_{31}^2 

Figure: Allowed values of Δm_{31}^2 at 3σ C.L. when SNSI is fitted in the theory with the standard three flavour scenario in the data.

Bounds

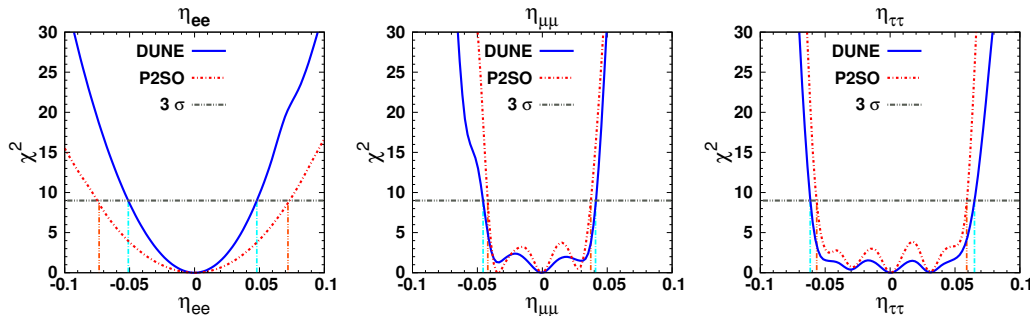


Figure: Bounds on the SNSI diagonal parameters (η_{ee} , $\eta_{\mu\mu}$ and $\eta_{\tau\tau}$) from DUNE and P2SO experiments.

Bounds

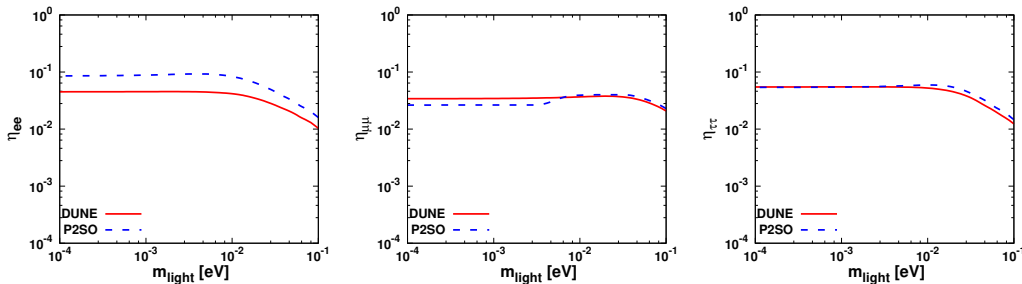


Figure: Constraints on scalar NSI parameters, η_{ee} (left), $\eta_{\mu\mu}$ (middle) and $\eta_{\tau\tau}$ (right) for DUNE and P2SO experiments in normal mass ordering.

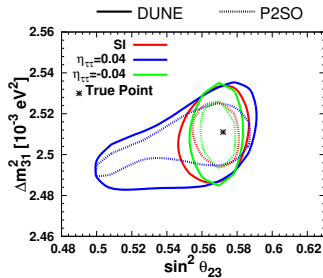
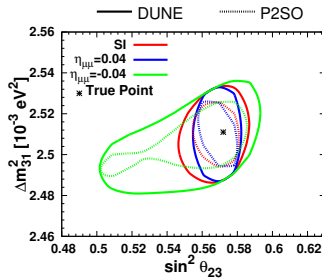
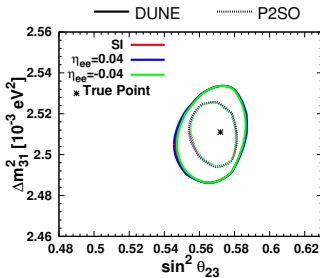


Figure: Allowed region between $\sin^2 \theta_{23} - \Delta m_{31}^2$ at 3σ C.L. in standard and in presence of SNSI parameters for DUNE and P2SO experiment.

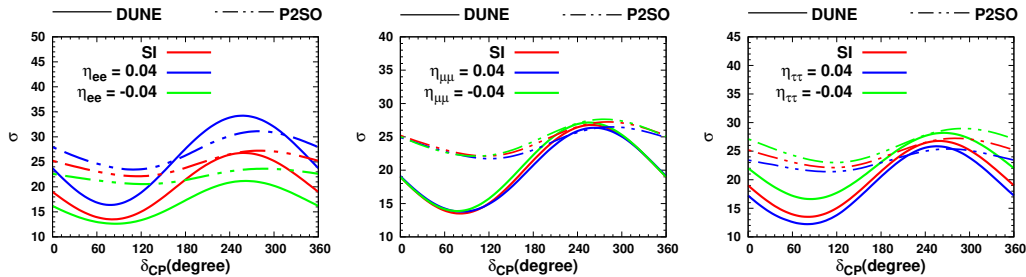


Figure: Mass hierarchy sensitivity of the SNSI diagonal parameters (η_{ee} , $\eta_{\mu\mu}$ and $\eta_{\tau\tau}$) for DUNE and P2SO experiment.

Events

Appearance channel event difference (Normal ordering - Inverted ordering)			
Experiments	$\eta = 0.04$	$\eta = 0$	$\eta = -0.04$
P2SO (η_{ee})	6992	6273	5609
DUNE (η_{ee})	360	244	150
P2SO ($\eta_{\tau\tau}$)	5336	6273	7510
DUNE ($\eta_{\tau\tau}$)	151	244	343

Table: Appearance channel event difference for P2SO and DUNE for $\delta_{CP}^{\text{true}} = 90^\circ$. These events corresponds to 3 years running of P2SO and 6.5 year running of DUNE.

Probability Formula in the presence of η_{ee}

$$\begin{aligned} P_{\mu e} = & \cos^2(\theta_{13} + \theta'_{13}) \cos^2 \theta_{23} \sin^2 2\theta'_{12} \sin^2 \left(\frac{\Delta_{21}^{\text{eff}} L}{2} \right) + \frac{1}{16} \sin^2 2(\theta_{13} + \theta'_{13}) \sin^2 \theta_{23} \\ & \times \left\{ 7 + \cos(\Delta_{21}^{\text{eff}} L) - 4 \cos((\Delta_{21}^{\text{eff}} - \Delta_{31}^{\text{eff}})L) - 4 \cos(\Delta_{31}^{\text{eff}} L) + 2 \cos 4\theta'_{12} \sin^2 \left(\frac{\Delta_{21}^{\text{eff}} L}{2} \right) \right. \\ & \left. - 8 \cos 2\theta'_{12} \sin \left(\frac{\Delta_{21}^{\text{eff}} L}{2} \right) \sin \left(\frac{(\Delta_{21}^{\text{eff}} - 2\Delta_{31}^{\text{eff}})L}{2} \right) \right\} + P_{\mu e}^{\delta_{CP}} \end{aligned} \quad (1)$$

where $P_{\mu e}^{\delta_{CP}}$ is the CP phase dependent part and is expressed as

$$\begin{aligned} P_{\mu e}^{\delta_{CP}} = & \cos^2(\theta_{13} + \theta'_{13}) \sin(2\theta_{23}) \sin(\theta_{13} + \theta'_{13}) \sin(2\theta'_{12}) \sin \left(\frac{\Delta_{21}^{\text{eff}} L}{2} \right) \\ & \times \left[\cos \delta_{CP} \cos 2\theta'_{12} \sin \left(\frac{\Delta_{21}^{\text{eff}} L}{2} \right) - \cos \left(\frac{\Delta_{21}^{\text{eff}} L}{2} \right) \sin \delta_{CP} + \sin \left(\delta_{CP} + \Delta_{31}^{\text{eff}} L - \frac{\Delta_{21}^{\text{eff}} L}{2} \right) \right] \end{aligned} \quad (2)$$

Probability features

$$\sin 2\theta'_{12} \sim 0 \implies a_{12} = 0.$$

This in turn gives

$$\eta_{ee} = \frac{-2\Delta m_{21}^2}{\sqrt{\Delta m_{31}^2(m_2 - m_1)(1 + \cos 2\theta_{13} - \sin 2\theta_{13} \tan \theta'_{13})}}. \quad (3)$$

If we assume the contribution to θ'_{13} to be negligible, then we will get $\eta_{ee} \sim -0.1748$.

$$2\theta'_{13}(\eta_{ee} = -0.1) = 1.61^\circ, \quad 2\theta'_{13}(\eta_{ee} = 0) = 3.56^\circ, \quad 2\theta'_{13}(\eta_{ee} = 0.1) = 6.02^\circ,$$

and hence we can conclude that

$$P_{\mu e}(\eta_{ee} < 0) < P_{\mu e}(\eta_{ee} = 0) < P_{\mu e}(\eta_{ee} > 0). \quad (4)$$

Probability features

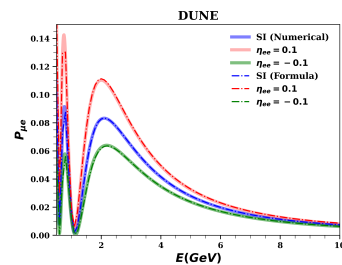
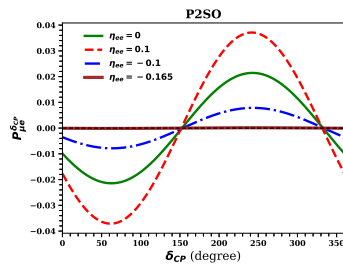
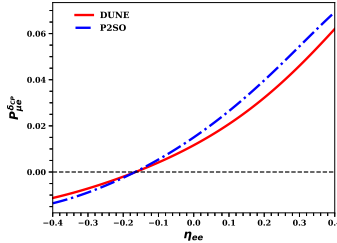


Figure: $P_{\mu e}^{\delta_{CP}}$ vs η_{ee} (left panel), $P_{\mu e}^{\delta_{CP}}$ vs δ_{CP} (middle panel) and $P_{\mu e}$ vs E (right panel).



Summary

- The change in probability amplitude depends on the relative sign of the SNSI parameter.
- Δm_{31}^2 has a non-trivial role for $\eta_{\mu\mu}$ and $\eta_{\tau\tau}$, bounds on these parameters depend on how Δm_{31}^2 is minimized.
- P2SO and DUNE are sensitive to absolute neutrino mass in the presence of SNSI.
- Sensitivity to η remains unchanged for $m_{light} < 10^{-2}$ eV.
- For certain values of η_{ee} , experiments become insensitive to δ_{CP} .

References

- B. Dutta, S. Ghosh, K. J. Kelly, T. Li, A. Thompson, and A. Verma, Non-standard neutrino interactions mediated by a light scalar at DUNE, arXiv:2401.02107.
- S.-F. Ge and S. J. Parke, Scalar Nonstandard Interactions in Neutrino Oscillation, Phys. Rev. Lett. 122 (2019), no. 21 211801, [arXiv:1812.08376].
- A. Medhi, M. M. Devi, and D. Dutta, Imprints of scalar NSI on the CP-violation sensitivity using synergy among DUNE, T2HK and T2HKK, JHEP 01 (2023) 079, [arXiv:2209.05287].
- K. S. Babu, G. Chauhan, and P. S. Bhupal Dev, Neutrino nonstandard interactions via light scalars in the Earth, Sun, supernovae, and the early Universe, Phys. Rev. D 101 (2020), no. 9 095029, [arXiv:1912.13488].



Acknowledgments

Thank You

Acknowledgments:

- I acknowledge CMSD HPC facility of Univ. of Hyderabad to carry out computations in this work.
- I acknowledge PMRF.

Backup Slides

Systematics	P2O	Up P2O	P2SO	DUNE
Sg-norm ν_e	7%	7%	5%	2%
Sg-norm ν_μ	5%	5%	5%	5%
Bg-norm	12%	12%	12%	5% to 20%
Sg-shape	11%	11%	11%	NA
Bg-shape	4% to 11%	4% to 11 %	4% to 11%	NA

Table: The values of systematic errors that we considered in our analysis. “norm” stands for normalization error, “Sg” stands for signal and “Bg” stands for background.

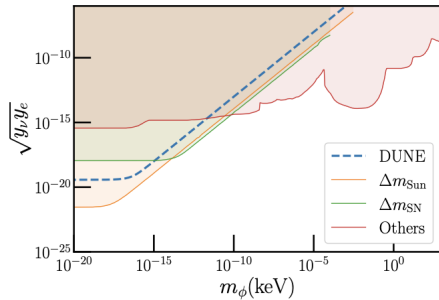
$$H_{SNSI} = E_\nu + \frac{\mathcal{M}\mathcal{M}^\dagger}{2E_\nu} + \text{diag}(\sqrt{2}G_F N_e, 0, 0) , \quad (5)$$

with

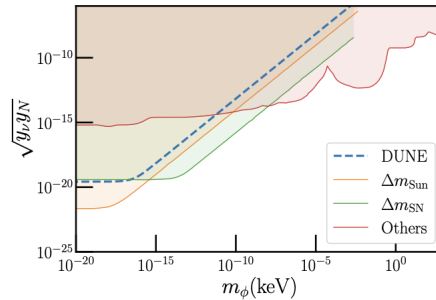
$$\mathcal{M} = U \text{ diag}(m_1, m_2, m_3) U^\dagger + \sqrt{|\Delta m_{31}^2|} \begin{pmatrix} \eta_{ee} & \eta_{e\mu} & \eta_{e\tau} \\ \eta_{\mu e} & \eta_{\mu\mu} & \eta_{\mu\tau} \\ \eta_{\tau e} & \eta_{\tau\mu} & \eta_{\tau\tau} \end{pmatrix} . \quad (6)$$

Whereas the same Hamiltonian in the presence of VNSI parameters ϵ can be written as:

$$H_{VNSI} = E_\nu + \frac{1}{2E_\nu} U \text{ diag}(m_1^2, m_2^2, m_3^2) U^\dagger + \sqrt{2}G_F N_e \begin{pmatrix} 1 + \epsilon_{ee} & \epsilon_{e\mu} & \epsilon_{e\tau} \\ \epsilon_{\mu e} & \epsilon_{\mu\mu} & \epsilon_{\mu\tau} \\ \epsilon_{\tau e} & \epsilon_{\tau\mu} & \epsilon_{\tau\tau} \end{pmatrix} . \quad (7)$$



(a)



(b)

χ^2 Analysis

We simulate the true (N^{true}) and test (N^{test}) event rates and compare them by using binned χ^2 method defined in GLoBES, i.e.,

$$\chi_{\text{stat}}^2(\vec{p}_{\text{true}}, \vec{p}_{\text{test}}) = \sum_{i \in \text{bins}} 2 \left[N_i^{\text{test}} - N_i^{\text{true}} - N_i^{\text{true}} \ln \left(\frac{N_i^{\text{test}}}{N_i^{\text{true}}} \right) \right], \quad (8)$$

where \vec{p} stands for the array of standard neutrino oscillation parameters. However, for numerical evaluation of χ^2 , we also incorporate the systematic errors using the pull method, which is generally done with the help of nuisance parameters as discussed in the GLoBES manual.

$$\chi_{\text{stat}}^2(p_{\text{true}}, p_{\text{test}}) = \sum_{i \in \text{bins}} \frac{(N_i^{\text{true}} - N_i^{\text{test}})^2}{N_i^{\text{true}}} \quad (9)$$

$$\chi_{\zeta}^2(p_{\text{true}}, p_{\text{test}}) = \min_{\zeta} \left[\sum_{i \in \text{bins}} \frac{(N_i^{\text{true}} - N_i^{\text{test}})^2}{N_i^{\text{true}}} + \frac{\zeta^2}{\sigma_{\zeta}^2} \right] \quad (10)$$

Lagrangian density

$$\mathcal{L}_{NSI} = -2\sqrt{2}G_F \epsilon_{\alpha\beta}^{fC} (\bar{\nu}_\alpha \gamma^\mu P_L \nu_\beta) (\bar{f} \gamma_\mu P_C f), \quad (11)$$

$$\mathcal{L}_{SNSI} = \frac{y_f Y_{\alpha\beta}}{m_\phi^2} (\bar{\nu}_\alpha \nu_\beta) (\bar{f} f), \quad (12)$$

where $y_f \rightarrow$ yukawa coupling between scalar and matter fermion, $Y_{\alpha\beta} \rightarrow$ yukawa coupling between scalar and propagating neutrino

Dirac equation

In general

$$\overline{\nu_\beta} [i\gamma^\mu (\partial_\mu + \text{vector contribution}) + (M_{\beta\alpha} + \text{scalar contribution})] \nu_\alpha = 0$$

For scalar NSI

$$\overline{\nu_\beta} [i\gamma^\mu \partial_\mu + (M_{\beta\alpha} + \frac{n_f y_f Y_{\alpha\beta}}{m_\phi^2})] \nu_\alpha = 0$$

S3 Extended seesaw particle content

Fields	e_R^c, μ_R^c	τ_R^c	$L_{1,2}$	L_3	$N_{R_{1,2}}^c$	$N_{R_3}^c$	ν_s	$H_{u,d}$	(Y_2^2)	(Y_2^4)	(Y_2^6)	(Y_1^8)	(Y_1^4)
$SU(2)_L$	1	1	2	2	1	1	1	2	-	-	-	-	-
$U(1)_Y$	1	1	-1/2	-1/2	0	0	0	$\pm 1/2$	-	-	-	-	-
S_3	2	1	2	1	2	1	1	1	2	2	2	1	1
K_I	1	-1	1	1	1	3	5	0	2	4	6	8	4

$$m_\nu^{3\times 3} = M_D M_R^{-1} M_S^T (M_S M_R^{-1} M_S^T)^{-1} M_S (M_R^{-1})^T M_D^T - M_D M_R^{-1} M_D^T \quad (13)$$

CPV

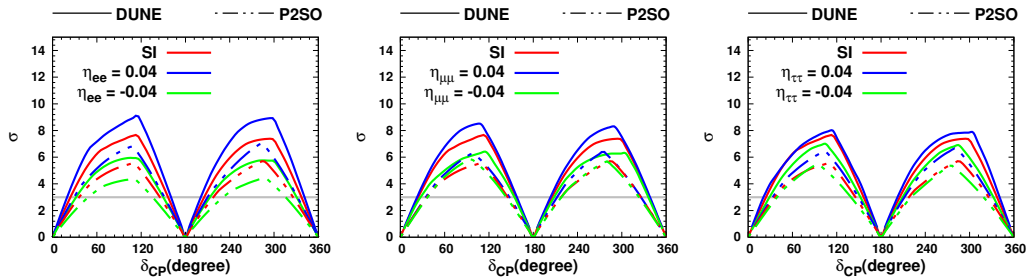


Figure: CPV sensitivity of the SNSI diagonal parameters (η_{ee} , $\eta_{\mu\mu}$ and $\eta_{\tau\tau}$) for DUNE and P2SO experiment.

Octant

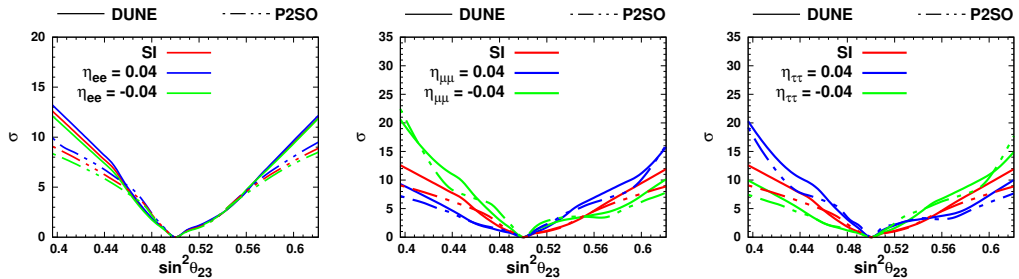


Figure: Octant sensitivity of the SNSI diagonal parameters (η_{ee} , $\eta_{\mu\mu}$ and $\eta_{\tau\tau}$) for DUNE and P2SO experiments.

Formula dependencies

$$\sin 2\theta'_{13} = \frac{a_{13}}{\sqrt{a_{13}^2 + b_{13}^2}} \quad (14)$$

where

$$\begin{aligned} a_{13} &= \left[2V_m + 2\Delta m_{31}^2 \eta_{ee}^2 + (m_1 + m_2 + 2m_3) \sqrt{\Delta m_{31}^2} \eta_{ee} + \sqrt{\Delta m_{31}^2} \eta_{ee} (m_1 - m_2) \cos 2\theta_{12} \right] \sin 2\theta_{13}, \\ b_{13} &= 2 \left[\Delta m_{31}^2 - \Delta m_{21}^2 \sin^2 \theta_{12} - V_m \cos 2\theta_{13} + 2m_3 \sqrt{\Delta m_{31}^2} \eta_{ee} \sin^2 \theta_{13} \right. \\ &\quad \left. - \Delta m_{31}^2 \eta_{ee}^2 \cos 2\theta_{13} - 2\sqrt{\Delta m_{31}^2} \eta_{ee} \cos^2 \theta_{13} (m_1 \cos^2 \theta_{12} + m_2 \sin^2 \theta_{12}) \right]. \end{aligned} \quad (15)$$

$$\sin 2\theta'_{12} = \frac{-a_{12}}{\sqrt{a_{12}^2 + b_{12}^2}}, \quad (16)$$

where,

$$\begin{aligned}
 a_{12} &= \sin 2\theta_{12} \left[2\Delta m_{21}^2 \cos \theta'_{13} + \sqrt{\Delta m_{31}^2} \eta_{ee} (m_2 - m_1) (\cos \theta'_{13} + \cos(2\theta_{13} + \theta'_{13})) \right], \\
 b_{12} &= 2 \left\{ -\cos^2 \theta_{12} \left(\Delta m_{21}^2 - 2\sqrt{\Delta m_{31}^2} m_1 \eta_{ee} \cos \theta_{13} \cos \theta'_{13} \cos(\theta_{13} + \theta'_{13}) \right) \right. \\
 &\quad + \cos^2 \theta'_{13} \left(\Delta m_{21}^2 \sin^2 \theta_{12} + \cos^2 \theta_{13} \left[\Delta m_{31}^2 \eta_{ee}^2 + V_m + 2\sqrt{\Delta m_{31}^2} \eta_{ee} m_2 \sin^2 \theta_{12} \right] \right) \\
 &\quad + \sin^2 \theta'_{13} \left(\Delta m_{31}^2 + \sin^2 \theta_{13} \left[\Delta m_{31}^2 \eta_{ee}^2 + V_m + 2\sqrt{\Delta m_{31}^2} \eta_{ee} m_3 \right] \right) \Big\} \\
 &- \frac{1}{2} \left[2\Delta m_{31}^2 \eta_{ee}^2 + \sqrt{\Delta m_{31}^2} \eta_{ee} (m_2 + 2m_3) + 2V_m \right. \\
 &\quad \left. - \sqrt{\Delta m_{31}^2} \eta_{ee} m_2 \cos 2\theta_{12} \right] \sin 2\theta_{13} \sin 2\theta'_{13}. \quad (17)
 \end{aligned}$$

$$\begin{aligned}
\Delta_{21}^{\text{eff}} = & \frac{1}{8E} \left[\cos 2\theta_{12}' \left\{ \Delta m_{21}^2 - 2\Delta m_{31}^2 \left(1 + \eta_{ee}^2 \right) - \sqrt{\Delta m_{31}^2} \eta_{ee} (m_1 + m_2 + 2m_3) \right. \right. \\
& - 2V_m + \left(2\Delta m_{31}^2 - \Delta m_{21}^2 \right) \cos 2\theta_{13}' - \sqrt{\Delta m_{31}^2} \eta_{ee} (m_1 + m_2 - 2m_3) \left(\cos 2\theta_{13} + \cos 2\theta_{13}' \right) \\
& - \left(2\Delta m_{31}^2 \eta_{ee}^2 + \sqrt{\Delta m_{31}^2} \eta_{ee} (m_1 + m_2 + 2m_3) + 2V_m \right) \cos 2(\theta_{13} + \theta_{13}') \\
& + \cos 2\theta_{12} \left[3\Delta m_{21}^2 + \sqrt{\Delta m_{31}^2} \eta_{ee} (m_2 - m_1) + \Delta m_{21}^2 \cos 2\theta_{13}' \right. \\
& \left. \left. + \sqrt{\Delta m_{31}^2} \eta_{ee} (m_2 - m_1) \left(\cos 2\theta_{13} + 2\cos\theta_{13}\cos(\theta_{13} + 2\theta_{13}') \right) \right] \right\} \\
& + 2 \left(\left[2\Delta m_{21}^2 + \sqrt{\Delta m_{31}^2} \eta_{ee} (m_2 - m_1) \right] \cos\theta_{13}' + \sqrt{\Delta m_{31}^2} \eta_{ee} (m_2 - m_1) \cos(2\theta_{13} + \theta_{13}') \right) \\
& \times \sin 2\theta_{12} \sin 2\theta_{12}', \tag{18}
\end{aligned}$$

$$\begin{aligned}
\Delta_{31}^{\text{eff}} = & \frac{1}{4E} \left[\left(\Delta m_{21}^2 + \sqrt{\Delta m_{31}^2} \eta_{ee} (m_2 - m_1) \cos^2 \theta_{13} \right) \cos \theta'_{13} \sin 2\theta_{12} \sin 2\theta'_{12} \right. \\
& + 2 \cos^2 \theta'_{13} \left(\Delta m_{31}^2 + \cos^2 \theta'_{12} \left[- \Delta m_{21}^2 \sin^2 \theta_{12} - \cos^2 \theta_{13} (\Delta m_{31}^2 \eta_{ee}^2 + V_m \right. \right. \\
& + 2\sqrt{\Delta m_{31}^2} \eta_{ee} (m_1 \cos^2 \theta_{12} + m_2 \sin^2 \theta_{12}) \left. \right] + \left[\Delta m_{31}^2 \eta_{ee}^2 + 2\sqrt{\Delta m_{31}^2} \eta_{ee} m_3 + V_m \right] \sin^2 \theta_{13} \left. \right) \\
& + \sin \theta'_{13} \left\{ \frac{1}{2} \sqrt{\Delta m_{31}^2} \eta_{ee} (m_1 - m_2) \sin 2\theta'_{12} \sin 2\theta_{12} \sin 2\theta_{13} \right. \\
& + 2 \left(\Delta m_{21}^2 \sin^2 \theta_{12} + \cos^2 \theta_{13} \left[\Delta m_{31}^2 \eta_{ee}^2 + V_m + 2\sqrt{\Delta m_{31}^2} \eta_{ee} m_2 \sin^2 \theta_{12} \right] \right) \sin \theta'_{13} \\
& - 2 \cos^2 \theta'_{12} \left(\Delta m_{31}^2 + \left[\Delta m_{31}^2 \eta_{ee}^2 + 2\sqrt{\Delta m_{31}^2} \eta_{ee} m_3 + V_m \right] \sin^2 \theta_{13} \right) \sin \theta'_{13} \left. \right\} + \left(1 + \cos^2 \theta'_{12} \right) \\
& \times \left(\Delta m_{31}^2 \eta_{ee}^2 + \sqrt{\Delta m_{31}^2} \eta_{ee} m_3 + V_m + \sqrt{\Delta m_{31}^2} \eta_{ee} m_2 \sin^2 \theta_{12} \right) \sin 2\theta_{13} \sin 2\theta'_{13} \\
& + \cos^2 \theta_{12} \left(- 2\Delta m_{21}^2 \sin^2 \theta'_{12} + \sqrt{\Delta m_{31}^2} \eta_{ee} m_1 \left(4 \cos^2 \theta_{13} \sin^2 \theta'_{13} \right. \right. \\
& \left. \left. + \left(1 + \cos^2 \theta'_{12} \right) \sin 2\theta_{13} \sin 2\theta'_{13} \right) \right) \left. \right]. \tag{19}
\end{aligned}$$